Deformation of Oriented Lamellar Block Copolymer Films

Yachin Cohen,[†] Ramon J. Albalak,[†,§] Benita J. Dair,[†] Malcolm S. Capel,[‡] and Edwin L. Thomas*[,†]

Department of Materials Science and Engineering, Massachusetts Institute of Technology, Cambridge, Massachusetts 02139, and National Synchrotron Light Source, Brookhaven National Laboratory, Upton, New York 11973

Received March 21, 2000; Revised Manuscript Received June 20, 2000

ABSTRACT: Highly ordered, near-single-crystal lamellar films of a triblock copolymer (polystyrene−polybutadiene−polystyrene, PS/PB/PS) were used to study the deformation mechanism of a structure of alternating glassy−rubbery layers, at different orientations of the deformation axis relative to the layer normal. Synchrotron radiation was used for simultaneous in-situ deformation and small-angle X-ray scattering measurements. These were augmented with direct imaging of the structure by transmission electron microscopy. The deformation mechanism depends on the orientation of the force with respect to the structure. Loading parallel to the lamellae results in yielding by propagation of a stable macroscopic neck. The glassy PS layers break up at the neck front, releasing the rubbery layers to achieve high strain. The morphology that develops by deformation of the structure in other directions is an ensemble of new tilt boundaries oriented along the deformation axis. The lamellar normals tilt away from the deformation axis with increasing strain, keeping the lamellar spacing essentially constant. The effect of force applied perpendicular to the lamellae is to fold the layers into a "chevron" morphology, similar to other layered systems such as smectic liquid crystals. At high strain, plastic deformation and fracture of the glassy PS hinges of the "chevron" structure leads to symmetric kink boundaries parallel to the force axis. In addition, nucleation of kink bands around defects and propagation of the kink boundaries into adjacent regions can lead to a similar morphology. The lamellar spacing remains constant during perpendicular stretching, and the tilt angle of the lamellar normal follows the macroscopic deformation in an affine manner. Stretching at 45° forms asymmetric kink boundaries parallel to the force axis. The major limbs of the kink band tilt with increasing strain so that the angle between the lamellar normal and the force axis increases from its initial value of 45°, while the lamellar period remains constant. The minor limbs tilt in the opposite direction and exhibit dilation of the lamellar spacing. Eventually the layers rupture, forming voids at the kink-boundary interfaces. The tilt angle of the major-limb lamellae, as a function of strain, is less than predicted by the affine model. This study suggests a general deformation mechanism for a lamellar structure of alternating glassy and rubbery layers. The layered structure responds to deformation, in any direction other then parallel to the layers, by creating new internal tilt-grain boundaries parallel to the deformation axis. At higher strain the layers yield and subsequently fracture at the kink-boundary interfaces. With increasing strain the lamellar stacks between the kink boundaries tilt toward the deformation axis until they are nearly parallel to it. Since the main features of this mechanism are independent of the initial orientation angle of the layers relative to the deformation axis, it is relevant also to polygranular, globally unoriented lamellar structures.

Introduction

Triblock copolymers that microphase separate into rubbery and glassy domains exhibit unique mechanical behavior ranging from that of thermoplastic elastomers to toughened thermoplastics. The microstructural basis for their mechanical properties has been studied extensively, as demonstrated in some recent reviews.[1−3] The solid-state structure can be viewed as a composite material having a periodic morphology with a length scale of tens of nanometers which depends on the chemical composition and length of the constituting blocks. Furthermore, the microphases are strongly interconnected since the covalently connected junctions between the constituent blocks are localized at their mutual interface.

This work is concerned with an A/B/A triblock copolymer of the glassy/rubbery/glassy type having a lamellar morphology. Most of the previous studies on such materials have been on macroscopically isotropic structures whereby the lamellar domains exist in a polygranular morphology without any overall preferred orientation. The main features of the unique mechanical behavior of lamellar block copolymer materials are as follows: (a) a linear elastic response with significant rigidity at low deformation up to a yield point; (b) yielding and drawing at higher deformations; (c) attainment of very large elongation; (d) large mechanical hysteresis and absorption of significant strain energy during the first mechanical cycle; (e) a plastic-to-rubber transition induced by high deformation so that subsequent strain cycles exhibit near-reversible rubber−elastic behavior; (f) healing upon unloading so that the original properties and microstructure are recovered upon annealing. This general behavior is also exhibited by the double-gyroid morphology when the glassy component forms the network.[4]

Previous deformation studies of lamellar block copolymer structures have led to important insight on the relevant phenomena. Fujimura et al.[5−7] studied the deformation of an unoriented lamellar structure of a PS/PB/PS triblock copolymer, which was spin-cast from solution, using small-angle X-ray scattering (SAXS) and transmission electron microscopy (TEM). Unstretched samples exhibited a multigrain lamellar morphology.

[†] Massachusetts Institute of Technology.
[‡] Brookhaven National Laboratory.
[§] Current address: Carmel-Olefins Ltd., Haifa, Israel.

10.1021/ma000513q CCC: $19.00
Published on Web 08/05/2000

Stretching beyond the yield point resulted in a chevron-like morphology with stacks of lamellae orienting such that their normals tilt away from the strain direction. This morphology was characterized by appearance of a four-point small-angle scattering pattern. The lamellar tilt angle increased continuously for strains increasing from 30% to 200%. Upon further stretching, the scattering pattern became diffuse, indicating a more random distribution of the lamellar fragments in the rubbery matrix. The morphological transitions in relation to the deformation process were discussed in terms of shearing, kinking, and breakup of the lamellae. At very high strain, a chaotic morphology was observed by TEM in which fragmented polystyrene domains appeared to be dispersed in the polybutadiene matrix. This breakup of glassy domains is termed the "plastic-to-rubber" transition.[5−7]

Séguéla and Prud'homme[8] used SAXS to study the deformation of an unoriented polystyrene−hydrogenated polybutadiene−polystyrene PS/hPB/PS triblock copolymer, which, despite its low PS content (29 wt %), microphase-separated to form lamellar microdomains. They also observed that the rings in the SAXS patterns typical of the isotropic polygranular structure before deformation were replaced by a four-point pattern at strains of 20% and above, associated with formation of a macroscopic neck. The angle between each arm of the four-point pattern and the equator remained close to 20° for strains ranging from 20% to 130%, and the *d* spacing was also nearly unchanged. This indicated a constant angle between the normal to the lamellae and the stretching direction during deformation, unlike the monotonic increase in the angle found by previous authors.[5−7] The deformation mechanism that was proposed invoked anisotropic grains of lamellae to rotate in response to the applied strain. As the long axis of these grains (termed the stacking axis) rotate toward the stretching direction with increasing strain, the lamellae are sheared relative to each other within the grains without appreciable change in their orientation.

Yamaoka and Kimura[9] studied a lamellar PS/PB/PS star-block copolymer processed by injection molding and by compression molding. Compression molding and subsequent rapid cooling resulted in oriented lamellar microdomains, whereas the samples produced by injection molding showed little orientation of the lamellae. Samples from both processes were fractured under tensile stress, and the morphology just below the fracture surface was studied using TEM. The randomly oriented lamellar grains of the injection molded sample were deformed by shear yielding, resulting in orientation of the domains at low strains. With increasing strain up to failure at about 600% strain, a morphology of fragmented PS domains dispersed in a PB matrix was observed. Stretching the oriented lamellae in the compression molded samples perpendicular to the lamellar planes resulted in the formation of a chevron-like morphology but without fragmentation of the PS domains. The authors also reported the formation of voids within the chevron morphology.

Allan et al.[10] used a unique injection molding technique to orient the lamellar microdomains in a PS−PB−PS triblock copolymer. After the molten material was injected into a mold, it was subjected to oscillatory shear by the reciprocating action of two pairs of pistons. They studied the low strain behavior of ensuing oriented lamellar structures, in the linear elastic regime, as a function of the angle between the lamellae and the applied stress. Their model assumed a homogeneous anisotropic material. The five elastic constants of the compliance tensor for this material were derived in terms of the moduli, volume fraction, and Poisson ratio of the individual rubbery (PB) and glassy (PS) layers using macroscopic composite mechanics. The anisotropy of Young's modulus was found to agree well with the model predictions, and the five elastic constants could be evaluated. In particular, the Young's modulus was found to have values of about 340, 130, and 900 MPa for deformations at angles of 0°, 45°, and 90° with respect to the lamellar normal.

Recently, a mechanical model for a layered block copolymer structure has been presented by Read et al.,[11] which treats in particular the response to deformation in the direction normal to the layers. They focus on the buckling of layers beyond a critical strain by an undulation instability which leads to folding of the layers into a "chevron" morphology. In their model, microscopic characteristics of the material are used, in addition to the macroscopic elastic constants of the homogeneous anisotropic body. These characteristics are the resistance to bending of the glassy layer and displacement of the rubbery layer relative to the glassy one, parallel to their common interface.

These previous studies have highlighted some main features of the microstructural basis of the mechanical response of lamellar block copolymer structures. However, deformation of globally unoriented or partially oriented structures involves a superposition of several deformation processes that occur simultaneously in regions that contain grains of lamellae at different angles with respect to the direction of deformation. The roll-casting technique[12−16] allows formation of a well-oriented "single-crystal"-like microstructure which can be subjected to deformation at well-defined angles of the lamellae relative to the direction of applied load. In this study we follow the microstructural transitions during room-temperature deformation of a near-single-crystal lamellar block copolymer structure, as a function of the angle between the applied force and the lamellar normal for both low and high strains.

Experimental Section

Films of a PS/PB/PS triblock copolymer were prepared from a commercial block copolymer, Vector grade 4461-D, manufactured by Dexco Polymers (12012 Wickchester, Houston, TX 77079). The molecular weight of each of the PS end blocks was 18 500, and that of the PB middle block was 45 000.[17] Vector 4461-D contains 45 wt % PS and microphase separates to form alternating layers of PS and PB.[15] Films were cast from toluene solutions containing 40 wt % polymer, using the roll-casting technique.[12−16] During the roll-casting process, a block copolymer solution is processed between rotating cylinders, while at the same time the solvent is evaporated at a controlled rate. As the solvent evaporates, the polymer concentration increases, and the block copolymer microphase-separates into a globally oriented morphology. For detailed information on roll casting we refer the reader to some of our other studies.[12−16]

Roll-cast films were dried in a vacuum oven at 50 °C for 48 h in order to remove all traces of the solvent. The films were then annealed at 120 °C for an additional 48 h. The lamellar alignment has been termed "perpendicular orientation" in studies of sheared diblock copolymer.[18−20] Samples for three types of stretching experiments were obtained by cutting the roll-cast film at different orientations, as shown in Figure 1. The axis notations are as follows: the *x* axis is the direction of the roll-casting flow field (tangential to the rolling cylinder),

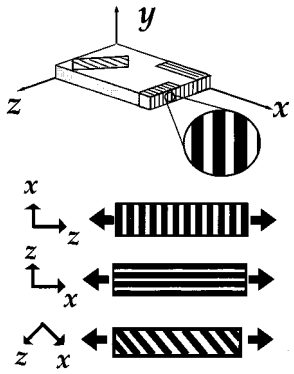

Figure 1. Schematic representation of a lamellar block copolymer film obtained by the roll-casting process. The axis notation: *x* axis is the flow direction (tangential to the rollers); *y* axis is the gradient direction (radial to the rollers); *z* axis is the neutral direction. Samples were cut from the roll cast film for deformation experiments at different angles between the lamellar normal and the deformation axis: 0° (perpendicular stretch), 90° (parallel stretch), 45° (diagonal stretch).

the *y* axis is the direction normal to the film surface (radial to the rolling cylinder), and *z* is the third (neutral) direction. Thus, samples for mechanical testing were obtained with the lamella normal oriented at 0°, 45°, and 90° relative to the stretching directions (*z* axis in Figure 1). These are termed as perpendicular, diagonal, and parallel stretching experiments, respectively.

The microstructural changes in the roll-cast films during deformation were monitored using small-angle X-ray scattering at the National Synchrotron Light Source (Brookhaven National Laboratory). Experiments were performed at a wavelength of $\lambda_x = 0.154$ nm at the Time-Resolved Diffraction Facility (station X12B). A custom-built two-dimensional gas delay-line detector (10 × 10 cm, 512 × 512 pixels) was used, interfaced to a real-time histogramming memory system.[21] The sample-to-detector distance was 222 cm. In these experiments the 1.2 mm thick films were continuously stretched in a custom-built tensile stage with an attached load cell. The dimensions of the test samples were 1.35 × 1.2 × 12.7 mm, and a crosshead speed of 2.6 mm/min was used. X-ray scattering patterns were recorded at different times at an exposure time of 15 s, except for the perpendicular stretch at strains above 250% where the exposure time was 30 s. The strain characteristic of a given exposure was taken as the median strain during that exposure. At the end of the deformation experiment, the sample was unloaded, and an additional SAXS pattern was recorded at zero load. SAXS data are presented as a function of the scattering vector $q = (4\pi/\lambda_x) \sin \theta$, where 2θ is the scattering angle and λ_x is the X-ray wavelength.

Tensile stress−strain characteristics were obtained from the stretching device used for the SAXS measurements as well as from separate uniaxial extension measurements using an Instron 4501 apparatus. Crosshead speeds of 2.6 and 1 mm/min were used, the latter being used to evaluate the initial modulus at low strains. For each orientation, an average of data from at least five samples is reported.

Real-space observation of the morphology in the stretched state was done using TEM. Samples in the perpendicular orientation stretched to 300% were cross-linked by electron irradiation (energy 2.6 MeV, dosage 200 Mrad) at the MIT High Voltage Laboratory. The residual strain upon release of the cross-linked sample was 170%. Samples in the diagonal orientation were cross-linked in the same way at 60% strain. In this case the strain did not change upon release of the sample. Thin sections were prepared by ultramicrotomy at −90 °C and were placed above a 4% aqueous solution of osmium tetroxide for 2 h to selectively stain the PB component. The stained sections were examined using a JEOL 2000 FX TEM operated at 200 kV. More details on the TEM technique are given elsewhere.[22−24]

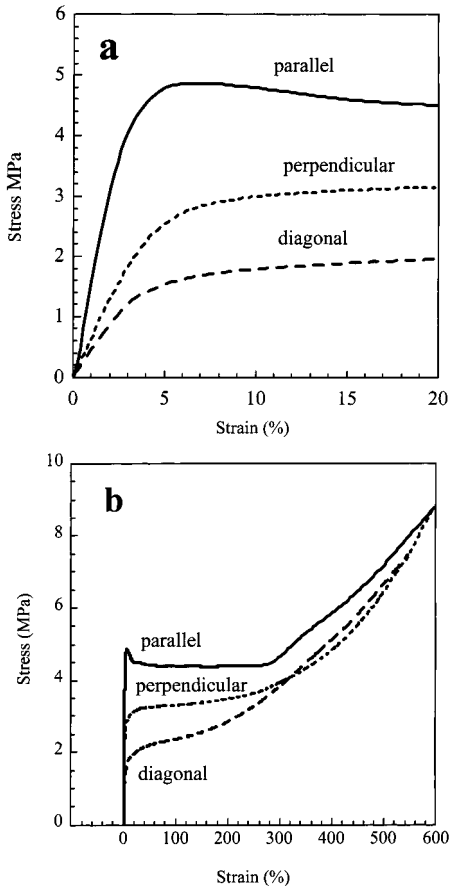

Figure 2. Stress−strain curves of oriented lamellar samples with the lamellar normal oriented at three directions relative to the deformation axis: solid line, 90° (parallel stretch); small-dashed line, 0° (perpendicular stretch); large-dashed line, 45° (diagonal stretch). (a) Low strain region; (b) high strain to break.

Results and Discussion

(a) Macroscopic Behavior. The mechanical response of highly ordered lamellar structures is presented by the stress−strain curves in Figure 2 for three different initial orientations of the lamellae relative to the stretching direction: parallel, perpendicular, and diagonal. The stresses and strains presented are in engineering units (load per initial cross-section area and length increment per initial length, respectively). At low strain, a reversible linear elastic response is observed, as shown in Figure 2a. The Young's moduli are 180 ± 10, 65 ± 3, and 43 ± 4 MPa for the parallel, perpendicular, and diagonal orientations. This anisotropy in modulus, with the diagonal orientation having the softest response, is in qualitative accord with the findings of Allan et al.[10] However, Allen et al.[10] report values that are larger by factors of about 5 for the parallel and perpendicular orientations and about 3 for the diagonal orientation. The experimentally measured moduli of the lamellar structure are very sensitive to the degree of orientation of the lamellae about the preferred axis. A higher degree of orientation increases the moduli in the parallel and perpendicular directions but would decrease the modulus in the diagonal direction. The molecular weight of the blocks as well as the sample geometry and measurement technique may also have an effect. Such details were not provided by Allan et al.[10]

Beyond the elastic region at low strain all samples exhibit a yielding behavior. For the parallel lamellar

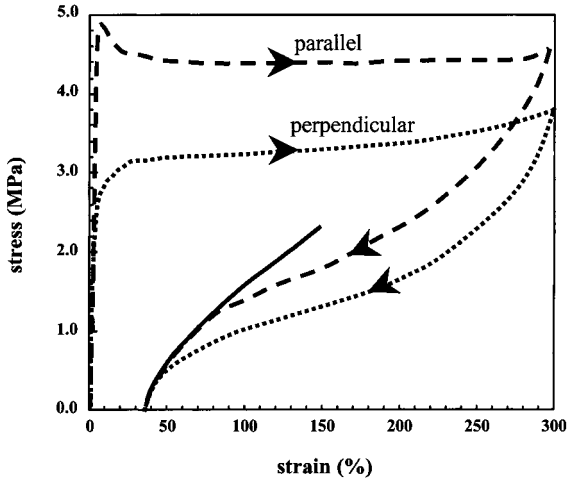

Figure 3. Stress−strain curves during loading of lamellar samples to 300% strain and subsequent unloading. Initial lamellar orientation relative to the stress direction: parallel (large-dashed line); perpendicular (small-dashed line); solid line: predicted curve for an ideal rubber with Young's modulus of 1.2 MPa.

orientation this is accompanied by distinct necking of the sample, often starting at one of the grips and traversing the length of the sample upon further deformation up to about 300% strain. The stable necking behavior is consistent with the drop in load observed in the stress−strain curve at the yield point (Figure 2). It is a consequence of the material having a relatively high yield stress and low strain hardening beyond the yield point.[25] During necking the dimensions of the sample cross section decreased to about 50−60% of the initial value in both lateral directions (y,z). Sample deformation in the direction perpendicular to the lamellae did not result in any noticeable necking. Rather, uniform drawing of the sample was observed, with its cross-section dimensions decreasing continuously in both x and y directions. It should be noted that unannealed samples behaved differently during perpendicular deformation. Distinct necking behavior was observed, with the sample dimensions decreasing only in the direction of the y axis. The different behavior of annealed and unannealed samples during perpendicular deformation will be discussed in a subsequent report.[26] Samples with the diagonal lamellar orientation also deformed uniformly, and no noticeable necking process could be observed.

At higher strain beyond yield, as shown in Figure 2b, the samples exhibit strain hardening. Thus, the mechanical response of the material during the initial deformation can be described as elastic-plastic. However, deformation to high strains transforms the material behavior from plastic to rubber-elastic. This transformation has been described for unoriented lamellar structures[5−7] as well as oriented block copolymer samples with cylindrical morphology.[27] Figure 3 shows the stress−strain curves measured during unloading after deformation to 200% in the parallel and perpendicular directions. Upon release of the load a residual strain of about 30% is measured in both cases. The mechanical behavior shown in Figure 3 is characteristic of a weakly cross-linked elastomer with a rigid filler. The elastic modulus obtained by fitting a standard rubber-elasticity model to the low-strain part of the curve for the parallel orientation, as shown in Figure 3, yields a modulus of about 1.2 MPa. This is reasonable for PB rubber having an entanglement molecular weight of about 2000.[2] Upon subsequent deformation the samples exhibit nearly reversible rubber-elastic behavior, each following its unloading curve in Figure 3.

(b) Microstructural Transformations. 1. The Initial Undeformed State. The roll-casting process achieves a high level of orientation and order in the lamellar block copolymer films. Further annealing above the glass-transition temperature of PS relaxes the residual stresses from processing and enhances the perfection of the level of ordering of the morphology.[15] Figure 4a shows the 2D SAXS pattern of an annealed roll-cast film of lamellar morphology before deformation. The SAXS pattern of the initial state exhibits sharp reflections with up to five discernible orders indicating a high degree of lamellar orientation perpendicular to the stretching direction with a lamellar period of 27 nm.

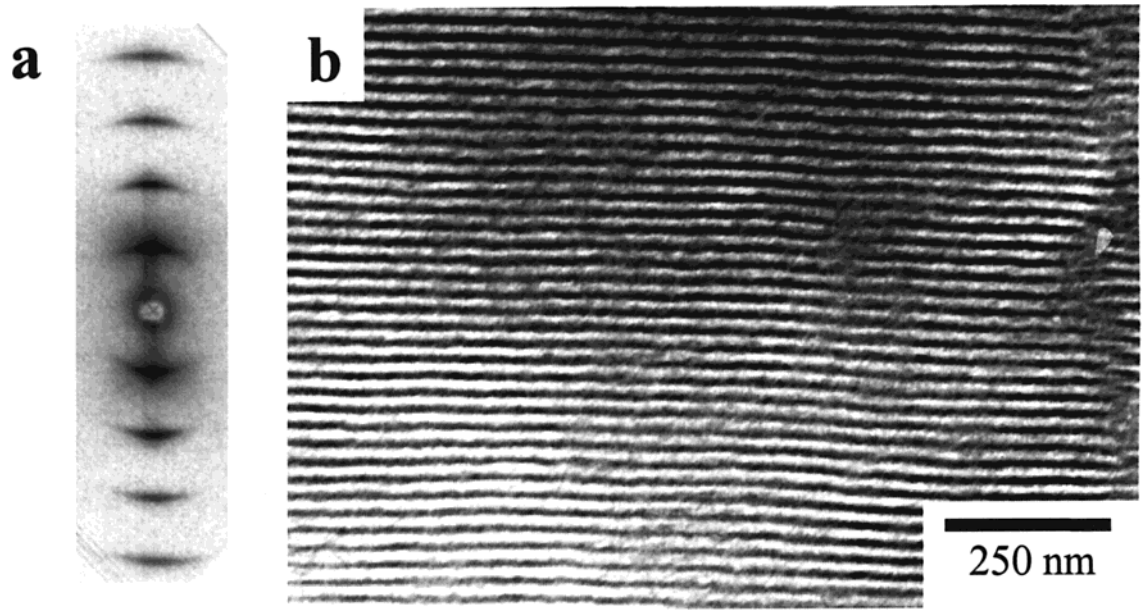

Figure 4. Morphology of the initial unstretched state: (a) SAXS pattern (intensity represented on logarithmic scale); (b) TEM image of the initial state of a textured block copolymer.

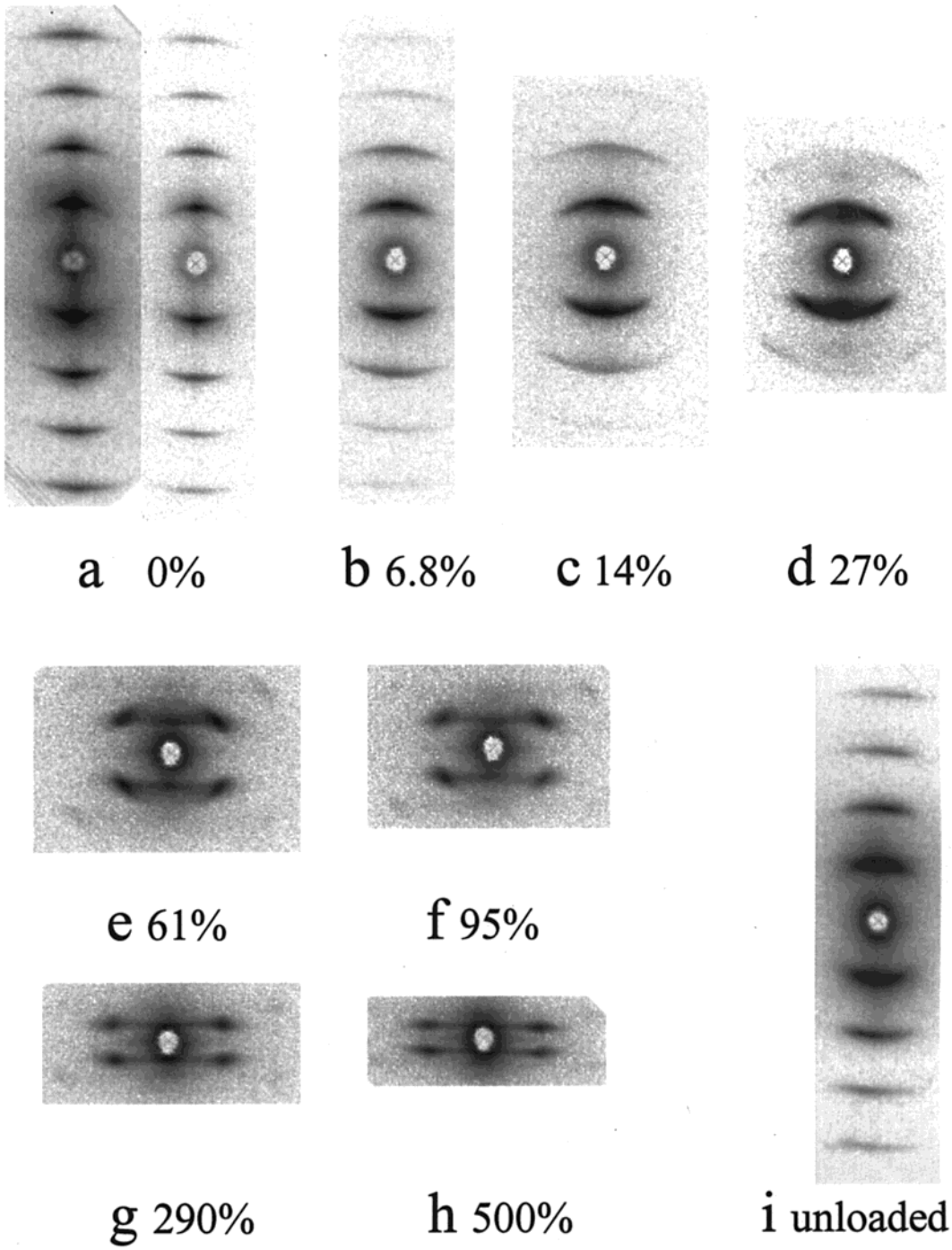

Figure 5. SAXS patterns obtained during deformation of a lamellar sample, with the load applied parallel to the lamellar normal ("perpendicular deformation"), at the following strains: (a) unstrained, (b) 6.8%, (c) 14%, (d) 27%, (e) 61%, (f) 95%, (g) 290%, (h) 500%, (i) unloaded to zero stress. Intensities are represented on a logarithmic scale, and the deformation axis is vertical.

The degree of misorientation, evaluated from the azimuthal spread of the (001) reflection, is ±5° (full width at half the maximum intensity: fwhm = 10°). The initial morphology in the undeformed state is presented in the TEM image in Figure 4b. It demonstrates the high degree of order and orientation achieved by the processing method. The structure is a coherent packing of lamellae across the sample without distinct grain boundaries. The lamellae have some waviness, and there are numerous edge dislocations ($\rho \approx 10^8/\text{cm}^2$), with Burgers vector magnitude equal to the lamellar period, located throughout the structure. Only a few cases were observed, in which the imaged region may suggest other defects such as screw dislocations or twist grain boundaries.[28] Tilt grain boundaries were not observed.

2. Perpendicular Deformation. Results of SAXS Measurements. Two-dimensional SAXS patterns representative of the deformation process along the *z* axis, with the incident X-ray beam parallel to the *y* axis of the film, are presented in Figure 5. Figure 5a shows the pattern of an annealed roll-cast film of lamellar morphology before deformation. For this particular run, a total of 71 patterns were recorded during deformation up to 600% and subsequent unloading. Selected patterns for nominal strains of 6.8, 14, 27, 61, 95, 290, and 500% are shown in Figure 5b−h. Figure 5i shows the SAXS

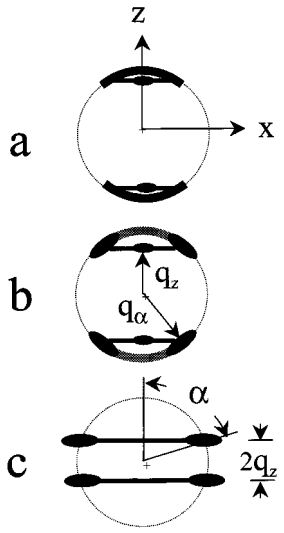

Figure 6. Schematic representations of the (001) reflections in the 2D SAXS patterns, observed during perpendicular stretching: (a) arcing at low deformation and the beginning of a meridional streak; (b) initial observation of a four-point SAXS pattern with tilted reflections, at intermediate strain; (c) fully developed four-point SAXS reflections, oriented along the meridional layer line. q_α is the scattering vector to a four-point reflection, where α is the angle between the reflection and the deformation axis, and q_z is its projection on the deformation axis (z).

pattern recorded immediately after unloading the sample at the end of the deformation experiment, in which a residual strain of 42% was measured. These are the nominal strains $\epsilon = \Delta L/L_0$, where L_0 and ΔL are the initial sample length and its incremental change upon deformation, respectively. This sample did not exhibit macroscopic necking although distinct yielding behavior was determined by simultaneous in-situ measurement of the load-extension curve, which was similar to that shown as the solid line in Figure 2.

Upon deformation, the scattering patterns can be divided into three types, which are shown schematically in Figure 6a−c. The main features at low strain (up to about 30% strain) are arcing of the (00l) reflections in the azimuthal direction and weakening of the higher order reflections, while the lamellar period remains approximately constant. It is difficult to discern any internal redistribution of intensity within the arc, but the overall shape of the (001) reflection suggests an arced reflection superimposed with a weak meridional reflection centered on a streak parallel to the equator (x direction). This can be seen in Figure 5d and is depicted schematically in Figure 6a. At deformations above about 30%, a second type of pattern appears where the intensity distribution along the arc of the 001 reflection clearly exhibits two maxima at specific azimuthal angles, with the eventual appearance of a characteristic four-point pattern, as depicted schematically in Figure 6b. Finally, at high deformations (Figure 5g,h) a third type of pattern occurs wherein the reflections of the four-point pattern have become elongated along the direction of the meridional layer line, as shown schematically in Figure 6c. We use the following notation for the reflections of the four-point patterns, as shown in Figure 6: α denotes the angle between the reflection and the meridian (z axis), q_α is the scattering vector, and q_z is its projection onto the z axis, for which the corresponding d spacings are denoted d and d_z, respectively. It is also evident that the layer line streak and the four-point reflections have a similar value of q_z which decreases in value (increasing d_z) with increasing deformation. The most striking result of the SAXS patterns shown in Figure 5 is that q_α remains approximately constant throughout the deformation process up to very high strain, demonstrating that the lamellar spacing is not changed by deformation.

Layer Folding: Undulation and "Chevron" Morphologies. We now consider the microstructural interpretation of the transitions associated with deformation of the lamellar structure in the perpendicular direction. The first effect observed at low strain is increased arcing of the (00l) reflections with increasing strain, while keeping a constant d spacing, as observed in Figure 5b−d and represented schematically in Figure 6a. We consider two possible real-space morphological transformations, which can give rise to such an effect during stretching: reorientation of the individual lamellar grains and/or undulation of the lamellar structure within a given grain, keeping the overall grain orientation unchanged. TEM observations show that the lamellae are coherently packed essentially throughout the entire sample, and therefore the notion of grain rotation seems inappropriate. On the other hand, undulation of layered structures in response to an extensional force perpendicular to the layers is known or predicted to occur in several systems. Such undulations have been theoretically predicted for smectic liquid crystals[29−31] and observed by Delaye et al.[32] for a homeotropic slab of a smectic A liquid crystal under tension. Undulations were also theoretically predicted to occur in a lamellar diblock copolymer structure by application of a perpendicular strain in the melt state under weak[33,34] as well as strong[34] segregation limits. An undulation instability has been suggested to occur in a block copolymer melt under shear flow conditions, based on theoretical considerations[35] as well as experimental observations,[36] when the lamellae are perpendicular to the vorticity axis. Moreover, Read et al.[11] have recently shown both analytically and by a finite element model the existence of a critical undulation instability in a perfectly aligned lamellar block copolymer structure subjected to perpendicular deformation under constraining boundary conditions. This allows a significant part of the deformation to be accommodated by shearing of the rubbery layer between the bent glassy layers. This behavior resembles the sinusoidal buckling of layered structures in geological formations subjected to lateral compression.[37]

The undulation instability discussed above is a highly cooperative phenomenon of a single-crystal-like arrangement of layers between confining external boundaries. The sample boundary conditions force adjacent layers to maintain their parallel orientation. This limits the ability to undulate with a long wavelength, since for a given strain the larger amplitude associated with a longer undulation wavelength necessitates significant dilation of the layers near the external boundary to which they must be parallel. Thus, the sample distance between the imposed boundary conditions is important in determining the critical strain and wavelength of the undulation instability. Although the degree of order achieved by our roll-casting process is high, the actual sample is far from being an ideal macroscopic single crystal as envisioned for the liquid crystal systems. The correlation distance along the lamellar normal, for which the layers are coherently packed, is clearly not the macroscopic distance between the grips of a tensile

stretching experiment. Furthermore, it is important to consider the effect of local defects in the ordered lamellar structure such as the edge dislocations. The layers in the vicinity of such defects are slightly misaligned and may be the first to respond to the applied stress by rotation of the lamellar normal away from the deformation axis. Opposite rotation of layers in the vicinity of defects may result in nucleation of kink bands. Kink bands can also form in misaligned regions around defects by a shear instability due to the resolved in-plane component of the applied stress.[25] With increasing strain, the kink bands propagate parallel to the deformation axis into neighboring layers.

The detailed mechanism of the transformation from the initial layered structure to the "chevron" morphology during perpendicular stretching, in relation to changes in the stress−strain behavior, is an important outstanding issue. The simulation of the undulation instability by Read et al.[11] associates the yield point of the stress−strain curve with the instability. This suggests that deformation in the linear elastic regime at low strain takes place by dilation of the layers. From their data a critical strain of at least 2% can be estimated. Our SAXS measurements do not show evidence for layer dilation at low (<20%) strain. Rather, increased arcing of the (001) reflection is observed. For example, the fwhm increases from 10° in the initial state to 16° and 28° for 7% and 15% strain, respectively. Within this range of strain, which covers the downturn in slope of the stress−strain curve, the spacing of the (001) arc at the meridional peak increases less than 0.5%. Even at 600% deformation the lamellar spacing, as measured from the four-point SAXS pattern, increases less than 2%. Thus, in regions where the lamellar normals are misoriented relative to the stretching direction, the applied strain is accommodated by further tilting of the normal. As discussed below for the case of the diagonal stretching experiment, this can be achieved by forming internal kink bands or undulations. No abrupt change in the character of the SAXS patterns could be associated with the yield point at about 5−10% strain. A more detailed study of the low-strain behavior is currently under way. It may be suggested that, below the yield point, tilting of the lamellae is confined to regions of misalignment such as those surrounding edge dislocations or other defects. Beyond the yield point, lamellar undulations occur in the entire sample as the stress exceeds the critical value for the undulation instability or that kink bands nucleated at the defect regions have propagated throughout the entire sample.

With increasing strain a four-point SAXS pattern is observed, as can be seen clearly in Figure 5e,f and illustrated schematically in Figure 6b. Such a four-point pattern has been associated with folding of the layers into a "chevron" morphology.[3,5−8] Figure 7a illustrates the folding of undulating layers into a "chevron" morphology where the layer contour is predominantly in the form of straight "limbs" and bending of the layers is localized to "hinge" regions. Figure 7b shows that such a pattern can already be observed at a strain as low as 27%, and it appears distinct at higher strain (e.g., 61% shown in Figure 7c). The transition from sinusoidal undulations to a "chevron" morphology has been treated analytically by Bayly[38] from a continuum mechanics point of view, applicable to layered geological structures, and by Singer[39] in the framework of the mesoscopic model, applicable to smectic liquid crystals and striped

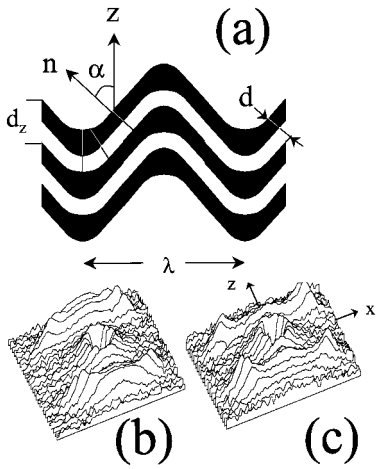

Figure 7. "Chevron" morphology: (a) a schematic representation of a few adjacent layers in a "chevron" morphology at a relatively high tilt angle α of the lamellar normal *n* relative to the deformation axis *z*; *d* and d_z are the lamellar repeat lengths in the tilted limbs and in the hinge regions, respectively. λ is the undulation wavelength. Surface plot representations of the 2D SAXS patterns at 27% (b) and 61% (c) strain.

magnetic patterns.[40] However, in both cases the layer spacing changed with deformation. Our measurements show that the *d* spacing of the four-point SAXS pattern remains constant with deformation. The rather sharp reflections suggest that a significant part of the contour of an undulating lamella is a straight limb with its normal tilted at a particular angle to the stretching direction. Adjacent limbs are connected by hinge regions of high curvature. At low strain the reflections of the four-point pattern are oriented along a circle of constant scattering vector. With increasing strain the tilt angle of these reflections flattens toward the meridional layer line. This may be due to narrowing of the hinge region and sharpening of the "chevron" angle with increasing strain. We also suggest that the weak meridional streak observed in the SAXS patterns is due to the thin hinge regions, where the layers are perpendicular to the stretching direction and have an increased lamellar spacing.[41] Figure 7a also depicts the PB layers in the hinge regions as being more dilated then the PS ones.

Formation of Kink Boundaries and Breakup of the Glassy Layers. At much higher strains (above about 300%) a different type of SAXS pattern appears, as shown in Figure 5g,h and schematically depicted in Figure 6c. In this case the reflections of the four-point pattern have become elongated along the direction of the meridional layer line. Such patterns have been observed in the deformation of unoriented lamellar block copolymers,[5−7] oriented cylindrical block copolymer structures,[3,42] and oriented semicrystalline lamellar structures.[43] This type of four-point pattern is due to a structure with grain boundaries parallel to the deformation direction, separating grains which are long in the stretching direction but narrow in the lateral direction. Within these long and narrow grains the diffracting entities are tilted. TEM observations provide direct evidence for this structure. Figures 8 depicts the TEM image of the structure in a lamellar sample stretched to 300% strain in the *z* direction perpendicular to the lamellae. The samples were cross-linked in the stretched state by electron irradiation, and the residual strain after unloading to zero stress was 170%. Staining with osmium tetroxide renders the PB phase dark in the TEM micrographs. The image of a section cut in the *y*−*z*

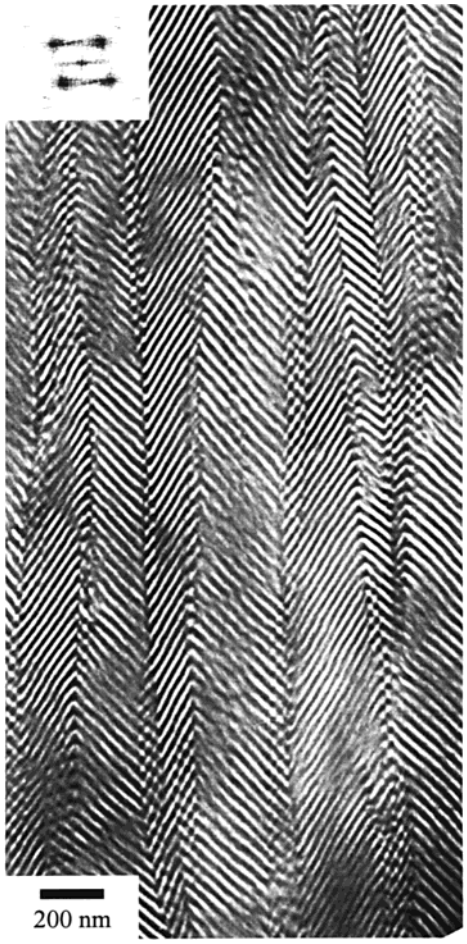

Figure 8. TEM image of a "chevron" structure formed by perpendicular deformation to 300% strain. Sample was cross-linked in the stretched state by electron irradiation. The residual strain immediately after release was 170%. Thins sections obtained by cryo-ultramicrotomy where stained with osmium tetroxide, rendering the PB phase dark in the image.

plane, shown in Figure 7, indeed verifies the appearance of a structure with many symmetric tilt grain boundaries parallel to the stretching direction. The tilt angle of the lamellar stacks alternates across the interface. The TEM image also shows that the number of lamellar repeat units along the lamellar normal direction between the kink boundaries is small (ca. 3−10) compared with the initial state. Therefore, no higher order reflections are observed in the four-point pattern of this structure, compared with the five orders of reflections in the initial undeformed structure.

The TEM image in Figure 8 clearly demonstrates that new kink boundaries have formed at high strain. The kink boundaries are a type of tilt grain boundary and are formed parallel to the direction of maximum extension, as has been shown in the cases of sheared[44−46] and extended[47] lamellar block copolymer melts. With increasing macroscopic strain, bending and dilation of the layers are increasingly localized to the thin "hinge" regions. Plastic deformation and eventual breaking of the glassy PS layers, which are bent at the hinge points, leads to formation of the new interfaces. Two kinds of tilt boundaries can be seen in Figures 8 and in the enlargements in Figures 9. Kink boundaries across which both layers are continuous, shown in Figure 9b, exhibit protrusions in the stained PB layer which resemble the "Ω" grain boundary. The "Ω" boundary, as well as "chevron" and "T-junction" types, was observed by Gido and Thomas[48] in melt-annealed polygranular lamellar samples. Its formation was ascribed to impingement of growing lamellar grains and molecular rearrangement at the grain boundary. This results in formation of two types of regions with protrusions of either the PB or the PS layers, as has been elaborated further by theoretical considerations.[49,50] In the present case of deformation at room temperature, the protrusions are observed *only* in the rubbery PB layers. This observation provides direct evidence for the localization of dilation in the rubbery PB phase at the hinge regions of the "chevron" structure. In the second type of kink boundary observed (see Figure 9a) both the PS and PB layers are discontinuous across portions of the boundary. These observations demonstrate that at about 300% strain the glassy PS layers at the kink boundaries have undergone major plastic deformation or have completely fractured.

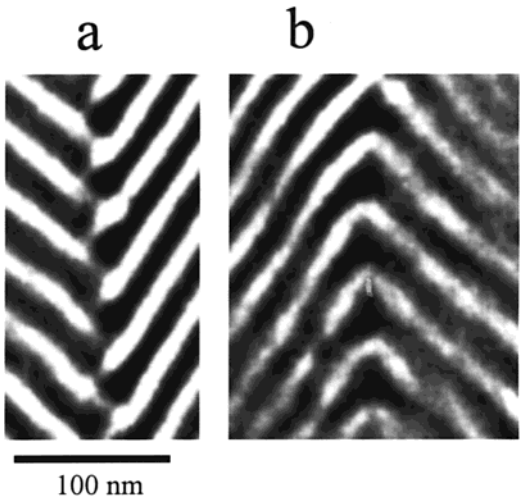

Figure 9. TEM images of tilt grain boundaries: (a) The "Ω" boundary formed by continuous PB and PS layers. Protrusions are observed only in the PB layers. (b) A tilt grain boundary across which the glassy PS layers are discontinuous.

We have considered two mechanisms for the transformation of the layered structure to the "chevron" structure and subsequently the morphology of alternating tilted lamellar stacks separated by tilt grain boundaries. Analogy to other layered systems such as smectic liquid crystals suggests the undulation instability model. We also suggest that tilting of the layers in regions surrounding defects such as edge dislocations nucleates local kink bands, which propagate into adjacent regions with increasing strain. The tilt grain boundaries propagate parallel to the applied force axis, eventually resulting in an array of variously spaced tilt boundaries, consistent with the TEM image in Figure 8. The length of a lamellar limb between the boundaries is in the range 0.5−1 μm. In the undulation instability model this distance is half the critical undulation and is expected to be regular. Furthermore, TEM images of longitudinal sections, such as the one shown in Figure 8, demonstrate that that the tilt grain boundaries formed in the deformation process are not always perfectly parallel and can be observed in some cases to impinge. Our current observations cannot distinguish the relative importance of these two mechanisms, and it is likely that both occur in the sample, depending on the degree of perfection of lamellar ordering in different regions.

The three-dimensional nature of the perpendicular deformation is indicated in Figure 10 which shows a top

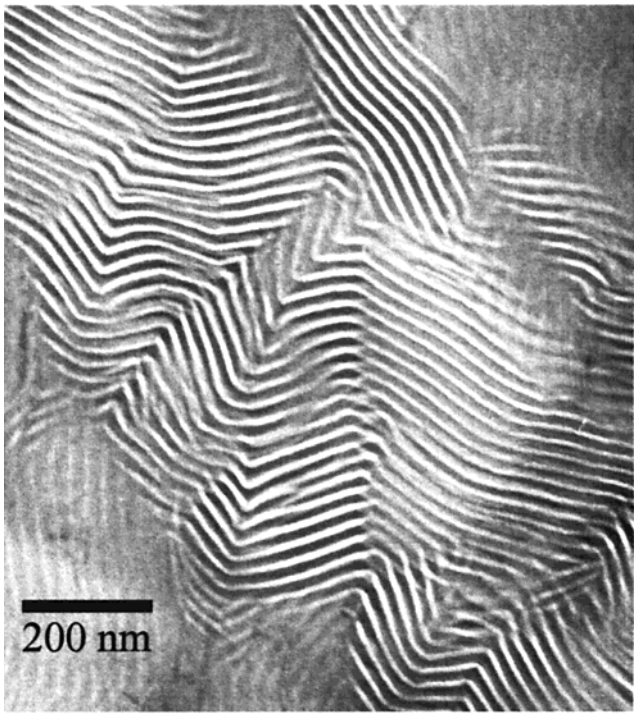

Figure 10. A TEM image showing a top view of the "chevron" structure taken from sections in the *xy* plane from a sample as in Figure 8.

view of the "chevron" structure taken from sections cut in the $x-y$ plane of a sample stretched to 300% then fixed by electron irradiation. The variously oriented regions of tilted lamellae indicate that the plane in which the lamellar normal tilts away from the *z* axis upon deformation is not regular. SAXS measurements from the well-annealed samples have shown chevron patterns and lamellar rotation about both the *x* and *y* axes. The initial morphology has uniaxial symmetry, which is preserved when the applied force is along the lamellar normal direction. Thus, any axis perpendicular to the direction of stretching is equally probable as a rotation axis, as verified by the combined SAXS and TEM observations. The particular axis about which the layers tilt likely depends on many factors such as the type, density, distribution, and orientation of defects in the lamellar packing and the degree of lamellar orientation along different axes. Most of these factors could not be evaluated or controlled in the present experiment.

Another issue related to the three-dimensional nature of the deformed structure needs to be addressed. In smectic liquid crystals it has been shown that buckling in the form of a "square-lattice" or "egg-box" morphology, where the layers fold simultaneously along perpendicular in-plane directions, has a lower energy than buckling along just one in-plane direction.[51,52] However, we have not seen evidence for such a regular "square-lattice" structure in TEM images taken with the projection direction along the *x* axis, such as Figure 10.

3. Diagonal Deformation. Insight into the very high deformation regime may be obtained by deformation experiments where the lamellae are initially oriented on average at a 45° angle to the stretching direction. The perpendicular deformation of the lamellar structure described above maintains uniaxial symmetry about the direction of applied force. This is not the case when the deformation axis is initially inclined at an oblique angle to the layered structure, where there is just one 2-fold symmetry axis, which is perpendicular to both the force direction and the lamellar normal. SAXS measurements were taken with the incident beam parallel to this symmetry axis. The SAXS patterns obtained in such a "diagonal" stretching experiment are shown in Figure 11. A schematic representation of the changes in the scattering pattern during diagonal deformation is given in Figure 12. At low strain, up to about 30%, the five reflections appear to move along arcs with the most intense portion of the reflection rotating at an increasing angle relative to the stretching direction (vertical in Figure 11). We denote the azimuthal angle between the stretching direction and the major (001) reflections as α_+. With increasing strain, as the major reflections rotate away from the stretching direction to larger values of the azimuthal angle, the arc of each reflection also extends to smaller values of the azimuthal angle. Thus, at 6.8% strain (Figure 11b) there is measurable intensity of the (001) arc on the meridian ($\alpha = 0$), at 27% strain (Figure 11c) there is measurable intensity at $\alpha < 0$, and at 61% strain (Figure 11d) a weak discrete reflection can be observed at negative α. The absolute value of the negative azimuthal angle between the stretching direction and this weak reflection is denoted α_-, as shown schematically in Figure 12. At higher strain, streaks appear through the (001) reflections, oriented perpendicular to the stretching direction. An equatorial streak through the origin can also be seen at high strain.

With increasing strain the (00*l*) reflections rotate to a larger angle from the stretching direction and their meridional spacing (d_z) increases. The *d* spacing to the (00*l*) reflections does not vary appreciably with deformation up to 500% strain. These observations are somewhat similar to what was observed in the perpendicular stretching experiment (Figure 5), where the observed four-point pattern is a superposition of two-point patterns with uniaxial symmetry about the stretching direction. The streaking of the reflections at low strain is due to nucleation and growth of kink boundaries. The TEM micrograph shown in Figure 13 provides direct evidence. This is an image of a microtomed section from the *xz* plane at 60% strain. The features evident in Figure 13 resemble thin kink bands which were shown to form in an oriented block copolymer melt, subjected to shear deformation parallel to the layers.[44−46] They are likely due to both components of the applied stress: shear parallel to the layers and tension in the perpendicular direction. These kink bands are very thin, and the tilt grain boundaries defining them are asymmetric. The lamellar limbs on one side of the boundary, the normal of which rotates away from stretching direction, are much larger than those within the kink band for which the normal rotates toward and past the stretching direction. Furthermore, the image in Figure 13 indicates that the latter lamellae, within the narrow kink band, have undergone significant dilation along the deformation axis as well as possible plastic deformation along the in-plane direction. At higher strain, with increasing tilt of the lamellar normal away from stretching direction, the short limbs in the narrow kink band undergo extensive in-plane deformation which leads first to breakup of the glassy layer and eventually even to rupture of the rubbery layers. At such high strain the *d* spacing to the weaker α_- reflection is again close to d_0, possibly due rupture at the kink-boundary interface which relaxes the dilational strain.

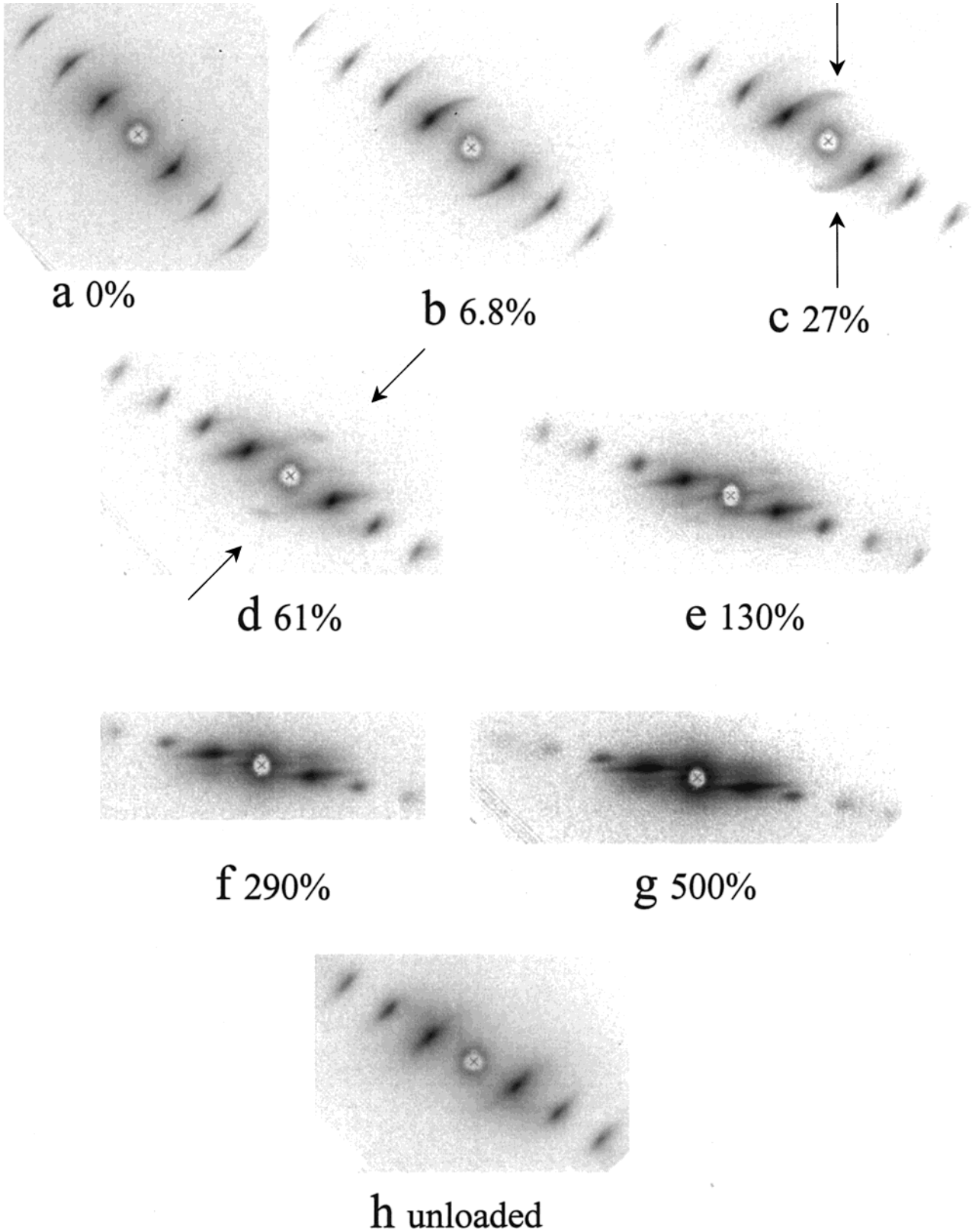

Figure 11. SAXS patterns obtained during deformation at an angle of 45° to the lamellar normal (the deformation axis is vertical), at the following strains: (a) unstrained, (b) 6.8%, (c) 27%, (d) 61%, (e) 130%, (f) 290%, (g) 500%, (h) unloaded to zero stress (intensities represented on a logarithmic scale). Arrows indicate α_- reflections.

The model for the response of the lamellar structure to diagonal strain is shown schematically in Figure 14. In this process new grain boundaries are formed parallel to the stretching direction. The layer line streaks observed in the SAXS patterns are due to the shape of the grains in which the tilted lamellae are stacked, which are elongated along the deformation axis and narrow in the transverse direction. This is qualitatively similar to what was described for perpendicular deformation. Retention of higher order reflections during diagonal deformation indicates a larger number of coherently packed lamellae between the kink bound-

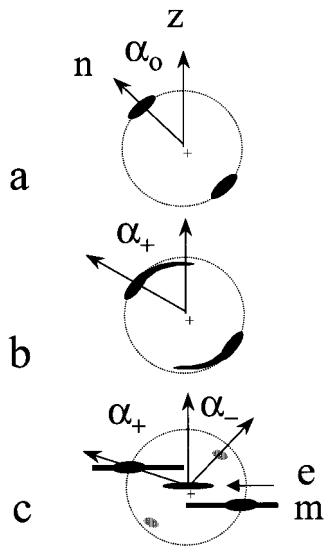

Figure 12. Schematic representations of the (001) reflections in the 2D SAXS patterns, observed during diagonal stretching: (a) the undeformed state; (b) rotation of the reflection at low strain to an azimuthal tilt angle α_+ between the reflection and the deformation axis; (c) the asymmetric four-point pattern with the major reflection at an azimuthal angle α_+, and the minor reflection at a negative azimuthal angle of magnitude α_-. Note the meridional and equatorial streaks (m and e, respectively).

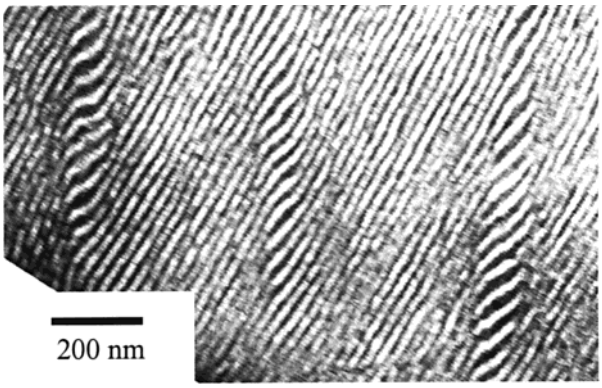

Figure 13. TEM image of kink bands formed by deformation at an angle of 45° to the lamellar normal (the deformation axis is vertical) to 60% strain. Sample preparation similar to that in Figure 8.

aries. Thus, the average lateral distance between kinks perpendicular to the deformation direction is larger than in the case of the "chevron" morphology. This model necessarily implies that continuity of the lamellae cannot be maintained across the newly formed boundaries. As the glassy layers break and rotate away the chains in the rubbery layers get extended, and eventually the polymer cavitates, forming a void. The equatorial streak in the SAXS patterns at high strain is consistent with formation of elongated voids in the stretching direction. Upon release of stress, a residual tilt of about 12° relative to the initial lamellar orientation is observed, as shown in Figure 11h.

4. Parallel Deformation. When the lamellar structure is deformed parallel to the lamellae (as in Figure 1b), the material exhibits the highest modulus and yield stress of all orientations. In this case symmetry of the system changes from uniaxial symmetry around the lamellar normal direction in the initial state to

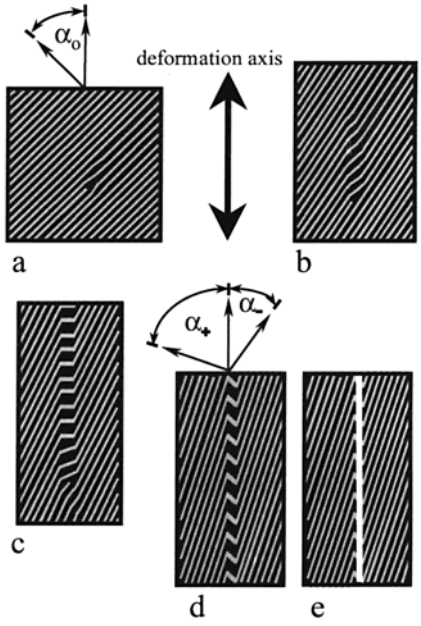

Figure 14. Schematic illustration of structural transformations during deformation at an angle of 45° to the lamellar normal: (a) the unstretched state; (b) kink band formation at relatively low strain; (c) fracture of the PS and PB layers at high strain and void formation at the kink boundary. Gray scale: black, PB; gray, PS; white, void.

2/*m*2/*m*2/*m* symmetry after application of the external load. SAXS measurements were obtained with the incident beam perpendicular to the directions of the applied force and the lamellar normal. The microstructural transitions during deformation, as seen from the SAXS patterns in Figure 15, are quite different from those discussed above for the perpendicular and diagonal stretching experiments. Figure 15a shows the two-dimensional SAXS pattern of the sample before deformation parallel to the lamellae. The patterns shown in Figure 15b−e were recorded at strains of 27%, 61%, 100%, 200%, and 290% respectively, with the deformation axis along the vertical direction. Figure 15f shows the SAXS pattern recorded after unloading the sample following a 400% strain. As mentioned earlier, during parallel deformation a stable macroscopic necking phenomenon is observed. Typically, a neck would form at one of the grips and transverse the length of the sample during the deformation process. The strains denoted in Figure 15 are therefore nominal values and are not the local strain at the point of measurement. The patterns in Figure 15b,c are from regions that were not necked, whereas the pattern in Figure 15e is from a location well into the neck. Figure 15d is from within the neck region. These observations were confirmed by measuring the SAXS patterns from a partially necked sample at a fixed macroscopic strain of 100% at different positions across the neck region. It is clear that necking destroys the ordered lamellar structure and that the sample at high strain contains thin voids elongated along the stretching direction.

The effect of low-strain deformation (Figure 15b,c) is 2θ broadening of the reflections, loss of higher order reflections, and appearance of a very diffuse reflection corresponding to a *d* spacing of about 24 nm. Below the yield point the applied stress results in some shearing of the lamellar structure such that the long period decreases. Beyond the yield point the glassy polystyrene layers break up into small fragments which allow the

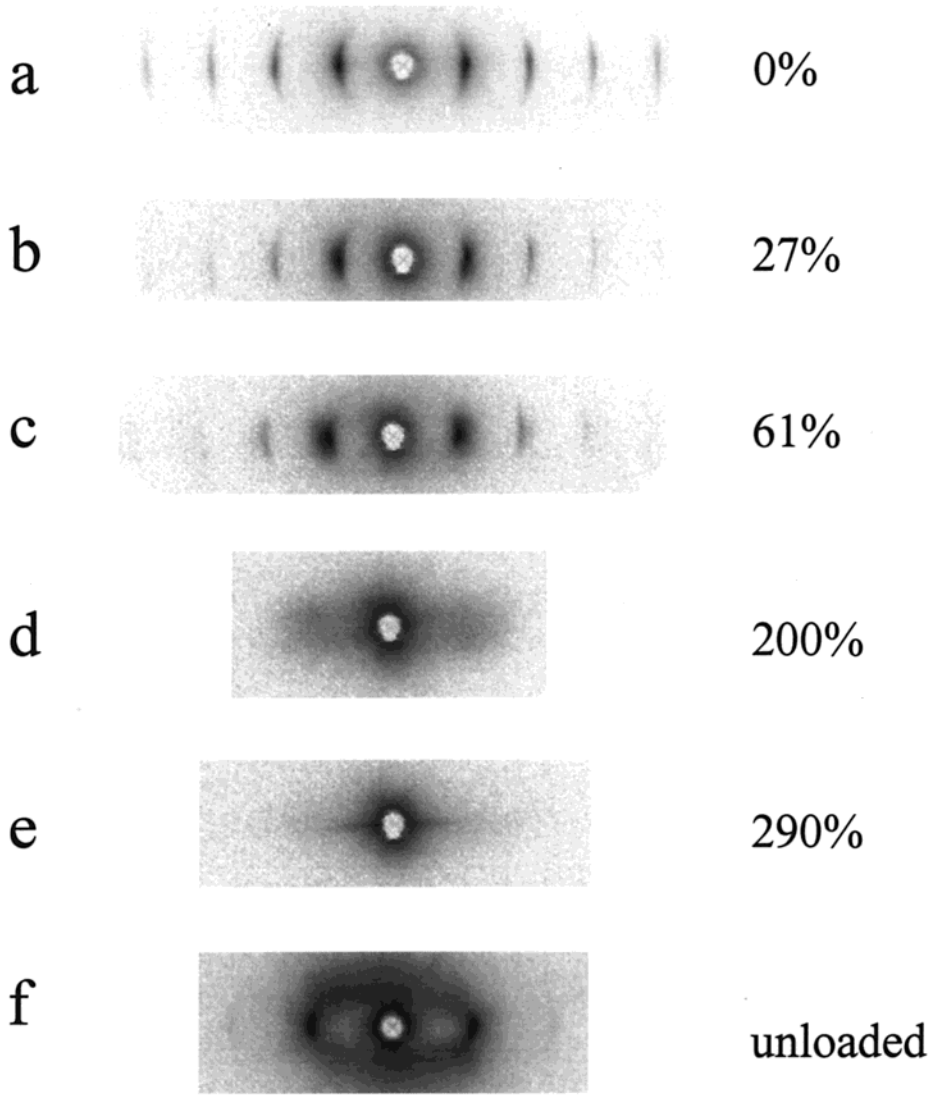

Figure 15. SAXS patterns obtained during deformation of a lamellar sample, with the load applied parallel to the lamellae, at the following nominal strains: (a) unstrained, (b) 27%, (c) 61%, (d) 200%, (e) 290%, (f) unloaded to zero stress. Intensities are represented on a logarithmic scale, and the deformation axis is vertical.

rubbery layers, now unconstrained by adjacent glassy layers, to deform elastically to a high level of strain. In this process elongated voids are formed between the polystyrene lamellar fragments. Lamellar fragmentation is localized at the front of the advancing neck, since that is the region of the lowest degree of order in the deforming lamellar structure. This is similar to previous observations on parallel deformation of a cylindrical block copolymer structure.[27] Also similar is the strain hardening at large deformations, associated with further fragmentation of the glassy remnants. A schematic representation of the destruction of the lamellar morphology in the neck region is presented in Figure 16. The SAXS pattern of the unloaded sample, shown in Figure 15f, has an elliptical shape with intense scattering along the equator. This suggests that the lamellar morphology has been reformed, albeit with a poor degree of orientation, and that the lamellar period depends on orientation. The spacing of the equatorial reflections, due to layers reformed in the original parallel orientation, is 20 nm. This value is smaller than the lamellar period in the initial state, possibly due to plastic deformation of the glassy lamellae during deformation.

(c) Analysis of Lamellar Tilting: The Affine Rotation Model. To evaluate the tilting of the lamellae with increasing strain, the average tilt angle $\langle\alpha\rangle$, obtained from SAXS measurements, is related to the macroscopic elongation $\lambda = L/L_0 = (1 + \epsilon)$. For the case of perpendicular deformation, consider a stack of lamellae having a repeat length d_0 and lateral dimension w in the unstrained reference state ($\lambda = 1$, $\alpha = 0$), viewed along a direction perpendicular to the stress axis and the lamellar normal, as shown in Figure 17. Upon deformation to an elongation λ, the lamellae tilt about an axis perpendicular to the stress direction so that the tilt angle obtains a value α, the lamellar repeat length is d, and the repeat length along the z axis is $d_z = d/\cos(\alpha)$. In the SAXS experiment, only the lamellae which tilt about an axis parallel to the incident beam maintain the diffraction condition. Measurements of the four-point SAXS patterns provide values of $\langle\alpha\rangle$, d ($=2\pi/q_\alpha$), and d_z ($=2\pi/q_z$) as a function of elongation, where q_α is the scattering vector to the reflection and q_z its projection along the deformation direction, as shown in Figure 6. We assume that the lateral dimension does not change upon rotation (w = constant) and

Figure 16. Schematic illustration of the fragmentation of the glassy PS lamellae during necking by deformation parallel to the lamellae. Gray scale: black, PB; gray, PS; white, void.

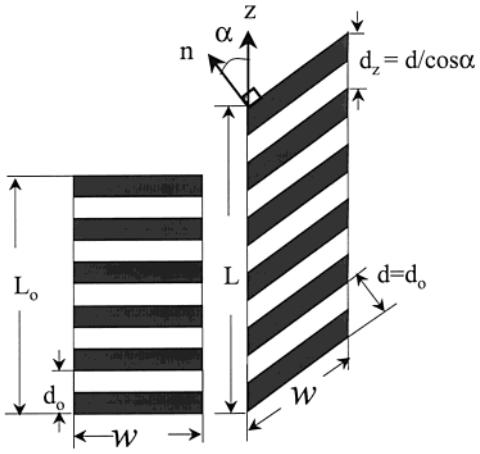

Figure 17. Schematic representation of the "affine rotation" model.

that volume is conserved during deformation (wd = constant), which leads to prediction of a constant d spacing of the four-point pattern during deformation ($d = d_0$ = constant). This can be viewed as simultaneous shear and dilation required to maintain constant volume of the deforming entity. If the lamellar stack contains a large number of lamellae, then the assumption of affine deformation relates the macroscopic elongation to microscopic dimensions as $\lambda = d_z/d_0$ so that[53]

$$1/\cos(\alpha) = \lambda \tag{1}$$

SAXS measurements show that the d spacing of the four-point reflections is constant at 27 nm throughout the deformation. Figure 18, where $1/\cos(\alpha)$ is plotted as a function of the elongation λ during deformation beyond the yield point, verifies that the rotation of the lamellae is affine with the macroscopic deformation.

When the layers in the initial state are tilted at an angle α_0 (e.g., $\alpha_0 = 45°$ for the diagonal stretching experiment), the analogous relation to eq 1 is

$$1/\cos(\alpha_+) = \lambda/\cos(\alpha_0) \tag{2}$$

Figure 19 shows a plot of $1/\cos(\alpha_+)$ as a function of

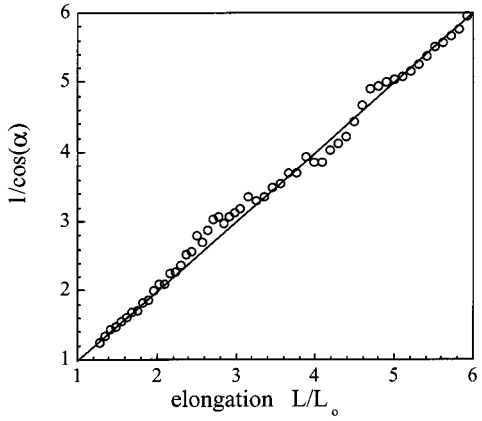

Figure 18. Test of the "affine rotation" model in the perpendicular deformation experiment. Relation of the tilt angle α measured by SAXS and plotted as 1/cos(α) to the macroscopic elongation $\lambda = L/L_0$. Solid line: the predicted linear relationship with unity slope passing through (1,1).

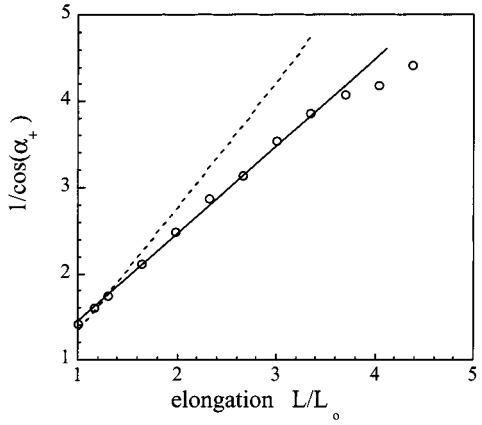

Figure 19. Test of the "affine rotation" model in the diagonal deformation experiment. Relation of the tilt angle α measured by SAXS and plotted as $1/\cos(\alpha_+)$ to the macroscopic elongation $\lambda = L/L_0$. Solid line: linear fit of the observed data (unity slope from point 1, 1.5). Dashed line: the predicted linear relationship with slope of $2^{1/2}$ passing through (1, $2^{1/2}$).

elongation for the diagonal stretching experiment. It can be seen that the relation of the tilt angle to elongation does not follow the affine rotation model (eq 2). Rather, an apparent linear relationship between $1/\cos(\alpha)$ and the macroscopic elongation with a slope near unity is observed. This indicates that tilting of the lamellae is less than expected by affine rotation. This may be rationalized on the basis of the microstructural observation discussed above. The TEM and SAXS experiments indicated that extensive dilatational deformation occurs in the narrow kink bands between stacks of tilted lamellae, the normals of which tilt away from the stretching direction. Eventually the layers within these regions fracture, forming a void or discontinuity between the tilting lamellar stacks. Furthermore, slippage may occur at these interfaces. If we assume that fraction of the elongation (denoted by ν) is taken up by processes other then lamellar tilting, then eq 2 should be modified as

$$1/\cos(\alpha) = (1 - \nu)\lambda/\cos(\alpha_o) \tag{3}$$

The near-unity slope of the measured data in Figure 19 indicates that about 30% of the applied strain is not effective in tilting of the lamellae. This is also in accord with the observed residual rotation of about 12° upon release of strain ($\cos 45°/\cos 57° \sim 1.3$).

Table 1. Deformation Mechanisms of a Lamellar Structure

orientation (α_0)[a]	macroscopic necking	low strain	high strain	affine rotation
parallel (90°)	yes	breakup of PS layers at yield	destruction of lamellar structure	not applicable
perpendicular (0°)	no[b]	layer undulation and "chevrons"	lamellar tilt, symmetric kink boundaries	yes
diagonal (45°)	no	asymmetric kink bands	lamellar tilt, void formation	no

[a] Angle between the lamellar normal and the deformation axis. [b] Unannealed samples did exhibit macroscopic necking.[26]

(d) Concluding Remarks. The achievement of highly oriented lamellar structures by the roll-casting process allowed evaluation of the microstructural basis for the macroscopic mechanical response of a lamellar block copolymer structure. The triblock copolymer material we studied is a nanoscale composite of alternating glassy and rubbery layers with molecular bonding between them. The deformation mechanism depends on the initial orientation of the lamellae relative to the deformation axis, as summarized in Table 1. Stretching parallel to the lamellae results in yielding by propagation of a stable macroscopic neck. The glassy PS layers break up at the neck front releasing the rubbery layers to achieve high strain, resulting in a plastic-to-rubber transition. The effect of loading perpendicular to the lamellae is similar to that observed in other layered systems such as smectic liquid crystals. Deformation leads to folding of the layered structure into a "chevron" morphology, and symmetric kink boundaries are formed at high strain. This can occur by both an undulation instability in very well ordered regions and nucleation of kink bands around defects with axial propagation of the kink boundaries. The tilt angle of the lamellar normal follows the macroscopic deformation in an affine manner for perpendicular deformation. In deformation at 45°, the tilt angle of the lamellae as a function of strain is somewhat smaller than expected by the affine model.

The morphology that develops due to deformation at any direction except parallel to the lamellae is an ensemble of new boundaries oriented along the deformation axis. Within these lamellar stacks the layer normals are tilted away from the deformation axis, and they continue to rotate with increasing strain, keeping the lamellar spacing essentially constant. The deformation morphology, which occurs when the loading axis is parallel to the lamellar normal, is symmetric with layers of comparable length and opposite sense of the tilt angle situated at each side of a narrow interface. When the initial state has the lamellae tilted at an angle to the stretching direction, as exemplified by the 45° stretching experiment, asymmetric kink boundaries are formed. Macroscopic yielding is due to microscopic yielding and eventually fracture of the layers at these boundaries. It is reasonable to conclude that a significant part of the energy during the yielding process is expended in formation of the new kink boundaries.

Stretching the material to very high strain leads to a transition from the initial elastic-plastic behavior to a reversible rubbery behavior. This results from the continued breakup of the glassy layers thus releasing the rubbery layers to deform in an unconstrained manner, in either shear or extension. At very high strains, the stress−strain curves of all three initial orientations coincide. Evidently at very high deformation (~600%) the morphology in all cases is similar—a highly stretched rubber matrix with anisotropic glassy reinforcements well oriented along the deformation axis. The rate of strain hardening at high deformation is related to continued fragmentation of the glassy reinforcement. Thus, it is more pronounced in the diagonal deformation where the initial lamellar fragments are the largest and hence can undergo more fragmentation at higher strain. During parallel deformation the PS layers are fragmented in the necking process to a smaller size, as indicated by the higher absorption of strain energy. During deformation to high strain, the glassy layers maintain their periodic spacing in the perpendicular and diagonal stretching experiments. Periodicity is destroyed, however, in the necking process during parallel deformation.

There are many similarities between the morphologies observed in deformation of the lamellar glassy−rubbery structure reported here and those observed in shear deformation of a lamellar block copolymer melt.[44−46] In both situations kink bands are nucleated with the kink boundaries parallel to the direction of maximum extension. With increasing strain, layer folding into "chevrons" with tilt and "Ω" boundaries is observed. At very high strain the PS layers at the kink boundaries fracture. Other features observed in melt-sheared samples,[46] such as elongation of the protrusions of the "Ω" boundaries along the shear direction, were not observed in our study. These features, which resemble the unbinding of dislocations,[40] require viscous flow in order to be formed in a block copolymer system.

The results reported here leave several questions related to deformation of structures composed of alternating glassy and rubbery layers unanswered. A major issue is the nature of the morphological response to perpendicular stretching at low strain. The deformation mechanism, whether an undulation instability or nucleation and propagation of kink boundaries, as well as its dependence on details of the initial lamellar structure, is currently under investigation. Furthermore, a better understanding of the three-dimensional nature of the ensuing morphology, and the compatibility of kink−kink interactions throughout the material, is subject to further investigations.

The results of this study are pertinent to the general case of globally unoriented lamellar structures. For an isotropic polygranular sample, most of the grains are initially oriented with their lamellar normal at an angle to the deformation axis, with a minority of grains having the lamellae either parallel or perpendicular to it. Thus, the prevalent mechanism is expected to be formation of new internal boundaries, parallel to the deformation axis, by undulation or kinking. Yielding and eventually fracture of the layers at the interfaces is followed by rotation of the tilted lamellar stacks toward the deformation axis up to high strain. When high deformation is achieved, the lamellae that have tilted to nearly parallel orientation can undergo further fragmentation, as in the case of parallel deformation.

Acknowledgment. This research was supported by Master Builders, Inc., the National Science Foundation (Grant NSF DMR 98-01759), and the MIT Center for

Materials Science and Engineering. The deformation device was constructed by Dr. C. Honeker (MIT) and is described in ref 22. Work at Brookhaven National Laboratory was supported by DOE. The triblock copolymer used was generously supplied by Dr. B. Walthers of Dexco Polymers. Helpful discussions with Prof. A. Argon, Prof. M. C. Boyce, Prof. R. J. Farris, and Dr. C. Honeker are gratefully acknowledged.

References and Notes

(1) Folkes, M. J. In *Processing Structure and Properties of Block Copolymers*; Folkes, M. J., Ed.; Elsevier: London, 1985; Chapter 4.
(2) Holden, G.; Legge, N. R. In *Thermoplastic Elastomers*, 2nd ed.; Holden, G., Legge, N. R., Quirk, R. P., Schroeder, H. E., Eds.; Hanser Publishers: New York, 1996; pp 48−69.
(3) Honeker, C. C.; Thomas, E. L. *Chem. Mater.* **1996**, *8*, 1702.
(4) Dair, B. J.; Honeker, C. C.; Alward, A. B.; Avgeropoulos, A.; Hadjichristidis, N.; Fetters, L. J.; Capel, M.; Thomas, E. L. *Macromolecules* **1999**, *32*, 8145.
(5) Fujimura, M.; Hashimoto, T.; Kawai, H. *Rubber Chem. Technol.* **1978**, *51*, 215.
(6) Hashimoto, T.; Fujimara, M.; Saito, K.; Kawai, H.; Diamant, J.; Shen, M. In *Multiphase Polymers*; Cooper, S. L., Estes, G. M., Eds.; ACS Advances in Chemistry Series; American Chemical Society: Washington, DC, 1979; pp 257−275.
(7) Kawai, H.; Hashimoto, T. *J. Macromol. Sci.* **1980**, *B17*, 427.
(8) Séguéla, R.; Prud'homme, J. *Macromolecules* **1981**, *14*, 197.
(9) Yamaoka, I.; Kimura, M. *Polymer* **1993**, *34*, 4399.
(10) Allan, P.; Arridge, R. G. C.; Ehtaiatkar, F.; Folkes, M. J. *J. Phys. D* **1991**, *24*, 1381.
(11) Read, D. J.; Duckett, R. A.; Sweeney, J.; McLeish, T. T. C. B. *J. Phys. D* **1999**, *32*, 2087.
(12) Albalak, R. J.; Thomas, E. L. *J. Polym. Sci., Polym. Phys. Ed.* **1993**, *31*, 37.
(13) Albalak, R. J.; Thomas, E. L. *J. Polym. Sci., Polym. Phys. Ed.* **1994**, *32*, 341.
(14) Albalak, R. J. *Polymer* **1994**, *35*, 4115.
(15) Albalak, R. J.; Thomas, E. L.; Capel, M. S. *Polymer* **1997**, *38*, 3819.
(16) Albalak, R. J.; Thomas, E. L.; Capel, M. S. *Polymer* **1998**, *39*, 1647.
(17) Reusche, D. A.; Lescanec, R. L. University of Southern Mississippi, unpublished results, 1995.
(18) Koppi, K. A.; Tirrell, M.; Bates, F. S.; Almdal, K.; Colby, R. H. *J. Phys. II* **1992**, *2*, 1941.
(19) Winey, K. I.; Patel, S. S.; Larson, R. G.; Watanabe, H. *Macromolecules* **1993**, *26*, 4373.
(20) Zhang, Y.; Wiesner, U.; Spiess, H. W. *Macromolecules* **1995**, *28*, 778.
(21) Capel, M. S.; Smith, G.; Yu, B. *Rev. Sci. Instrum.* **1995**, *66*, 2295.
(22) Honeker, C. C. Ph.D. Thesis, Massachusetts Institute of Technology, 1997.
(23) Dair, B. J. Ph.D. Thesis, Massachusetts Institute of Technology, 1999.
(24) Honeker, C. C.; Thomas, E. L. *Macromolecules*, submitted.
(25) McClintock, F. A.; Argon, A. S. *Mechanical Behavior of Materials*; Addison-Wesley: Reading, MA, 1996.
(26) Cohen, Y.; Thomas, E. L., manuscript in preparation.
(27) Odell, J. A.; Keller, A. *Polym. Eng. Sci.* **1977**, *17*, 544.
(28) Gido, S. P.; Gunther, J.; Thomas, E. L.; Hoffman, D. *Macromolecules* **1993**, *26*, 4506.
(29) De Gennes, P. G.; Prost, J. *The Physics of Liquid Crystals*; Clarendon Press: Oxford, 1993.
(30) Helfrich, W. *Appl. Phys. Lett.* **1970**, *17*, 531.
(31) Hurault, J. P. *J. Chem. Phys.* **1973**, *59*, 2086.
(32) Delaye, M.; Ribota, R.; Durand, G. *Phys. Lett.* **1973**, *A44*, 139.
(33) Amundson, K.; Helfand, E. *Macromolecules* **1993**, *26*, 1324.
(34) Wang, Z.-G. *J. Chem. Phys.* **1994**, *100*, 2298.
(35) Drolet, F.; Chen, P.; Vinals, J. *Macromolecules* **1999**, *32*, 8603.
(36) Wang, H.; Newstein, M. C.; Krishnan, A.; Balsara, N. P.; Garetz, B. A. *Macromolecules* **1999**, *32*, 3695.
(37) Johnson, A. M. *Styles of Folding;* Elsevier: New York, 1977.
(38) Bayly, M. B. *Technophysics* **1974**, *24*, 291.
(39) Singer, S. J. *Phys. Rev. E* **1993**, *48*, 2796.
(40) Seul, M.; Wolfe, R. *Phys. Rev. Lett.* **1992**, *68*, 2460.
(41) The streak may also be due to a different population of highly anisotropic lamellar grains having a large coherence length perpendicular to the lamellae and a very narrow one parallel to the lamellae. Such grains may be expected to be more resistant to buckling and hence would deform by simple uniaxial extension. However, we have not seen evidence for such grains by TEM.
(42) Pakula, T.; Saito, K.; Kawai, H.; Hashimoto, T. *Macromolecules* **1985**, *18*, 1294.
(43) Song, H. H.; Argon, A. S.; Cohen, R. E. *Macromolecules* **1990**, *23*, 870.
(44) Polis, D. L.; Winey, K. I. *Macromolecules* **1996**, *29*, 8180.
(45) Polis, D. L.; Winey, K. I. *Macromolecules* **1998**, *31*, 3617.
(46) Qiao, L.; Winey, K. I. *Macromolecules* **2000**, *33*, 851.
(47) Hudson, S. D.; Amundson, K. R.; Jeon, H. G.; Smith, S. D. *MRS Bull.* **1995**, *20*, 42.
(48) Gido, S.; Thomas, E. L *Macromolecules* **1994**, *27*, 6137.
(49) Matsen, M. W. *J. Chem. Phys.* **1997**, *107*, 8110.
(50) Netz, R. R.; Andelman, D.; Schick, M. *Phys. Rev. Lett.* **1997**, *79*, 1058.
(51) Delrieu, J. M. *J. Chem. Phys.* **1974**, *60*, 1081.
(52) Rosenblatt, C.; Pindak, R.; Clark, N. A.; Meyer, R. B. *J. Phys. (Paris)* **1977**, *38*, 1105.
(53) A similar relation is given in ref 39.

MA000513Q